DTIC FILE COPY

AD-A197 338

REPORT DOCUMENTATION PAGE

1a. REPORT SECURITY CLASSIFICATION: Unclassified	1b. RESTRICTIVE MARKINGS
2a. SECURITY CLASSIFICATION AUTHORITY	3. DISTRIBUTION/AVAILABILITY OF REPORT: Unlimited
2b. DECLASSIFICATION/DOWNGRADING SCHEDULE	
4. PERFORMING ORGANIZATION REPORT NUMBER(S): Technical Report No. 9	5. MONITORING ORGANIZATION REPORT NUMBER(S)
6a. NAME OF PERFORMING ORGANIZATION: The University of Texas at Arlington; 6b. OFFICE SYMBOL (If applicable)	7a. NAME OF MONITORING ORGANIZATION: Office of Naval Research
6c. ADDRESS (City, State, and ZIP Code): Department of Chemistry, Box 19065, The University of Texas at Arlington, Arlington, Texas 76019	7b. ADDRESS (City, State, and ZIP Code): 800 North Quincy Street, Arlington, Virginia 22217
8a. NAME OF FUNDING/SPONSORING ORGANIZATION: Defense Advanced Research Projects Agency; 8b. OFFICE SYMBOL (If applicable): DARPA	9. PROCUREMENT INSTRUMENT IDENTIFICATION NUMBER: N00014-86-K-0769
8c. ADDRESS (City, State, and ZIP Code): 1410 Wilson Boulevard, Arlington, Virginia 22209	10. SOURCE OF FUNDING NUMBERS: PROGRAM ELEMENT NO. / PROJECT NO. / TASK NO. / WORK UNIT ACCESSION NO.

DTIC ELECTE JUL 25 1988 S E

11. TITLE (Include Security Classification): Electronic and Ionic Transport in Polymers

12. PERSONAL AUTHOR(S): Charles K. Baker and John R. Reynolds

13a. TYPE OF REPORT	13b. TIME COVERED	14. DATE OF REPORT (Year, Month, Day)	15. PAGE COUNT
Technical	FROM _____ TO _____	1988 July 12	34

16. SUPPLEMENTARY NOTATION: Journal of Electroanalytical Chemistry, in press

17. COSATI CODES: FIELD	GROUP	SUB-GROUP

18. SUBJECT TERMS (Continue on reverse if necessary and identify by block number): Electroactive polymers, electropolymerization, quartz crystal microbalance.

19. ABSTRACT (Continue on reverse if necessary and identify by block number)

An electrochemical quartz crystal microbalance has been used to study the anodic electropolymerization of pyrrole and concurrent deposition of polypyrrole onto gold in acetonitrile and propylene carbonate using tetraethylammonium tosylate, tetrabutylammonium fluoroborate, and lithium perchlorate. Simultaneous dynamic measurements of charge and mass have been used to monitor the efficiency of the polymerization/deposition process as a function of film thickness and electrodeposition rate. This work demonstrates that the early stages of film formation is affected by the solubility of the oligomers formed and that the ultimate efficiency is electrolyte dependent. Additionally, it is shown that the polymerization process exhibits second order reaction kinetics with respect to monomer concentration.

20. DISTRIBUTION/AVAILABILITY OF ABSTRACT	21. ABSTRACT SECURITY CLASSIFICATION
☒ UNCLASSIFIED/UNLIMITED ☒ SAME AS RPT ☐ DTIC USERS	Unclassified
22a. NAME OF RESPONSIBLE INDIVIDUAL: Dr. John Millikan	22b. TELEPHONE (Include Area Code): (202-696-4410 ; 22c. OFFICE SYMBOL

DD FORM 1473, 84 MAR — 83 APR edition may be used until exhausted. All other editions are obsolete. SECURITY CLASSIFICATION OF THIS PAGE

A Quartz Microbalance Study of the Electrosynthesis of Polypyrrole

Charles K. Baker and John R. Reynolds*

A Contribution From the

Department of Chemistry
The University of Texas at Arlington
Arlington, TX 76019

ABSTRACT

An electrochemical quartz crystal microbalance has been used to study the anodic electropolymerization of pyrrole and concurrent deposition of polypyrrole onto gold in acetonitrile and propylene carbonate using tetraethylammonium tosylate, tetrabutylammonium fluoroborate, and lithium perchlorate. Simultaneous dynamic measurements of charge and mass have been used to monitor the efficiency of the polymerization/deposition process as a function of film thickness and electrodeposition rate. This work demonstrates that the early stages of film formation is affected by the solubility of the oligomers formed and that the ultimate efficiency is electrolyte dependent. Additionally, it is shown that the polymerization process exhibits second order reaction kinetics with respect to monomer concentration.

INTRODUCTION

The electrochemical synthesis of conducting polymers onto an existing electrode substrate has become a popular method of preparing polymer modified electrodes. There are many examples of aromatic and heterocyclic based monomers which can be electropolymerized and deposited onto a number of materials such as metals, indium tin oxide (ITO) on glass, and vitreous carbon [1]. The most studied of these heterocyclic containing electroactive polymers is polypyrrole. There are also a growing number of examples of polymerizations which are carried out within a pre-cast polymer matrix existing on these electrode materials resulting in an electroactive polymer composite [2]. While many studies have been published in attempts to elucidate the structure, electronic properties, and potential applications of these materials, only a few papers have addressed the mechanism of electropolymerization and the effects of polymerization conditions on the deposition process.

Investigations of the mechanism of polymer film deposition onto supporting electrode substrate of polythiophene, polypyrrole and poly(N-methylpyrrole) have been studied electrochemically using cyclic voltammetry (CV), chronocoulometry, chronoamperometry and optical absorption techniques [3-14]. Typical cyclic voltammograms of these monomers exhibit a single broad oxidation wave which is indicative of electron transfer followed by an irreversible chemical reaction. This oxidation produces a continuous insoluble conducting polymer film on the supporting electrode substrate, which exhibits electroactive properties that depend on film morphology, counter (or dopant) anions, and supporting electrolyte and can be electrochemically cycled between a "doped" conducting state when oxidized and a non-conducting neutral state. Additional oxidative scans or constant potential electrolyses in a monomer containing electrolyte solution can result in a free standing film which may be removed intact from the underlying electrode surface, typically Pt, Au, vitreous carbon, or indium-tin oxide. An important feature of the oxidation/polymerization process is found when the switching potential of the initial CV scan is lower than the monomer oxidation potential. This results in a return scan current which is higher than that seen during the forward oxidative scan. This is consistent with nucleation and growth of

a conducting surface phase on the electrode surface [3-14]. Potential step experiments of pyrrole and thiophene in acetonitrile and aqueous solvents yield current-time *i-t* curves with three distinct regions of behavior suggesting that there are three separate stages involved during film formation. The first stage is marked by a sharp initial current spike whose decay is potential dependent, non-exponential, and on time scales longer than expected if it were due to double layer charging [3, 4, 5], as seen in the case of metal deposition [6]. Rotating ring-disc electrode and coulometric experiments of thiophene deposition on gold by Hillman [5] indicates that this initial spike has a contribution from both a nucleation/growth process and formation of soluble oligomers. The amount of charge passed and duration of the spike suggest that the first stage in the *i-t* curves corresponds to the coverage of the metallic electrode by a one monolayer thick polymer film. A study by Marcos [7] using a Tafel slope analysis and measurement of Pt electrode surface coverage by adsorbed pyrrole monomer has yielded different ΔH values for pyrrole adsorbtion and polymerization on Pt (13.7 kJ mol^{-1}) and for pyrrole polymerization, or nucleation and growth, on the existing polypyrrole layer (17 kJ mol^{-1}). The second and third stages in the *i-t* curves are characterized by a rising charge transient, lasting from 1 to 5 seconds, followed by a steady constant current for the remainder of electropolymerization. During the rising portion of the curve i is proportional to t^2 which is indicative of instantaneous formation of nucleation sites on polymer monolayer (ΔH=17kJ mol^{-1}) followed by three-dimensional growth until these sites overlap. Once these sites coalesce, additional growth is thought to occur perpendicular to the substrate resulting in a linear increase in thickness with time.

Other theoretical and electrochemical studies involving the relationship between electropolymerization conditions and the properties of the resulting films have lead to conclusions about the efficiency and mechanism of the oxidation/deposition process. The picture that emerges from these studies indicates that the polymerization for the bulk of film formation is as shown in Scheme 1 for polypyrrole. Polymerization is initiated by the oxidation of monomer to yield a

Insert Scheme 1

radical-cation species. Although some [8] have suggested that the next step may be formation of a covalent bond between this radical-cation and a neutral monomer, followed by an electron transfer from this product, this seems unlikely because of the potential dependence found in the copolymerization of pyrrole with substituted pyrroles [15] and therefore the second step is more likely the coupling of radical-cations to yield dimers. These resulting dimers can then be oxidized at lower potentials [16] to yield a radical-cation dimers in which the highest spin density is found at the terminal carbons alpha to the pyrrole nitrogens. These dimer radical-ions, or at later stages, oligomers may couple with other radical-ion monomers, dimers, or oligomers eventually leading to an insoluble film. This lack of solubility is inherent to unsubstituted polymers containing a conjugated planar backbone. This planarity is due to the energy minima associated with the overlap of adjacent π-orbitals which is necessary to achieve efficient electron transport along the polymer chain. The insolubility of these materials limits the number of analytical techniques which can be employed for characterization. It seems likely that this decreasing solubility and oxidation potential with increasing molecular weight would affect the nature and efficiency of deposition when the electropolymerization process includes oligomers as well as monomer oxidation and coupling.

To study this problem, we have employed an electrochemical quartz crystal microbalance (EQCM) which can simultaneously perform *in-situ* electrochemical and gravimetric experiments [17-26]. The quartz crystal microbalance has been used for many years to determine mass changes of perfectly rigid metallic films in vacuum by monitoring changes in the resonant frequency (f) of an oscillating quartz crystal by using the Sauerbrey equation [27]:

$$\Delta f = - 2f_o^2 \Delta m / A(\rho_q \mu_q)^a \qquad (1)$$

where f_o = resonant frequency of the unloaded quartz crystal sandwiched between two metallic electrodes, m = change in mass in grams, A = surface area of electrode or film, ρ_q = density of the quartz = 2.648 g cm^{-3}, μ_q = shear modulus of quartz = 2.947 x 10^{11} dynes cm^{-2}. Recent work

has shown that when one face of an AT-cut quartz crystal, operating in the shear surface mode, is immersed in a liquid, the crystal will continue to oscillate with a constant frequency shift determined by the viscoelastic properties of the liquid overlayer:

$$\Delta f = - f_o^{3/2}(\rho_l \eta_l / \pi \rho_q \mu_q)^{1/2} \qquad (2)$$

where ρ_l and η_l are the density and absolute viscosity of the overlayer, respectively [28]. Thus when the face of the crystal is used as the working electrode in an electrochemical cell, as in our system, a frequency shift will be seen upon exposure to solution and any elastic solid material deposited on the electrode, which meets the criteria for a rigid film, can be treated with the Sauerbrey equation. In order to apply this equation to a polymer film in solution, the film must behave as a rigid, perfectly elastic overlayer. Studies on several polymer systems [17-21] as well as a rigorous derivation of the equations [29] indicate that this rigid film approximation is valid if the polymeric overlayer thickness is small compared to the thickness of the crystal and if the overall mass loading results in a frequency change that is small with respect to the resonant frequency of the unloaded crystal.

Since the EQCM retains a high sensitivity (18 ng cm^{-2} Hz^{-1}) in a solution environment, it has been used in studies of metal deposition onto, and dissolution from, an electrode [22], studies of monolayer coverage by oxygen and organic molecules on an electrode surface [23,24], and the characterization of morphological changes and surface reconstructions associated with electrode potential perturbations [25]. In addition to this ability to study the metal/electrolyte interface, redox processes occurring in electroactive polymeric materials deposited on an electrode surface have been monitored. The movement of ions and solvent molecules associated with charge transport in electronically conducting polymers has been studied for polypyrrole [17,18], the "self-doped" poly{pyrrole-co-[3-(pyrrol-1-yl)propanesulfonate]} [26], and polyaniline [21] as well as for the electroactive polymer, poly(vinylferrocene) [20].

EXPERIMENTAL

Electrochemical polymerization experiments were done using 0.1M tetraethylammonium tosylate (TEATOS) and tetrabutylammonium tetrafluoroborate ($TBABF_4$) with various concentrations of pyrrole in acetonitrile (CH_3CN) distilled from P_2O_5 under nitrogen and propylene carbonate distilled from $KMnO_4$ under nitrogen. The electrolytes were used as received. Pyrrole was purified by passing it over an alumina column until colorless in order to remove any oligomeric pyrrole species which occur from atmospheric oxidation. All potentials reported are versus a $Ag/AgNO_3$ (0.1 mol dm^{-3}) reference electrode.

A schematic of the electrochemical quartz crystal microbalance (EQCM) system used is shown in Figure 1. A 5 MHz AT-cut quartz crystal (Valpey-Fisher) was clamped via an o-ring seal such that the area exposed to solution (0.7 cm^2) is less than the area of oscillation. The oscillator/potentiostat circuit used is similar to that used by Melroy [22b] and was donated by IBM Research Division. This circuit uses a high gain differential amplifier with current feedback to drive the crystal to oscillate and, since one face of the crystal is grounded, it may be used as a working electrode in a Wenking type three-electrode potentiostat. The potential at the working electrode is set via a 12 bit digital-to-analog converter and the resulting current read via a 16 bit analog-to-digital converter both from a Tecmar Labmaster data acquisition and control PC add-on board. The resonant frequency of the quartz oscillator is measured using a Philips PM6654 frequency counter and sent via an IEEE-488 interface bus to an IBM PC which is used to control, obtain, process and store data from both the frequency counter and Tecmar Labmaster. Thus, our system can be used to generate any potential waveform desired and to measure both the resulting electrochemical and gravimetric response occurring at the electrode surface.

A typical electropolymerization experiment would include a solution of 0.1 mol dm^{-3} pyrrole and 0.1 mol dm^{-3} TEATOS in acetonitrile which has been deoxygenated by purging it with nitrogen for 15 minutes. A non-oxidative starting potential, usually 0.0 V *vs.* $Ag/AgNO_3$, was set

and held at the working electrode until the cell current and quartz oscillation frequency were stable. Typical values for prepolymerization frequency drift for a 5 MHz crystal in solution were 20 Hz hr^{-1} which corresponds to 2.5×10^{-7} g hr^{-1} with a resolution of 1 Hz or 1.2×10^{-8} g. The potential at the gold electrode was then stepped to a value on the oxidation wave found on a cyclic voltammogram of pyrrole monomer. Typical values for this step ranged from 0.6 to 1.0 V *vs.* $Ag/AgNO_3$. The current passed was measured via the analog-to-digital converter and the frequency by the frequency counter and sent to the IBM PC. The two data sources were sampled consecutively every 200-250 ms over the course of the experiment for approximately 5 minutes (or 1500 data points) with a delay between a frequency and current sampling of less than 1 ms. Total frequency changes due to deposition of polymer on the gold electrode for these experiments ranged from 30,000 to 60,000 Hz, or from 3 to 7 mg of polypyrrole, with the same resolution and drift as before the potential step. The frequency was used to calculate mass using the Sauerbrey equation and the current integrated using Simpson's rule to yield charge.

RESULTS

Effect of Pyrrole Concentration

A cyclic voltammogram for pyrrole monomer, Figure 2, shows an irreversible oxidation wave with an E_{pa} of 0.9 V. This behavior suggests the formation of an unstable radical-cation which can undergo further chemical reaction. Figure 3 shows frequency and charge *vs.* time for a typical constant potential polymerization in which the electrode polymer is stepped from 0.0 to 0.9 V in a CH_3CN solution containing 0.1 mol dm^{-3} TEATOS and 0.05 mol dm^{-3} pyrrole. To study the effect pyrrole monomer concentration has on the efficiency of electropolymerization, constant potential polymerizations were carried out where the charge and frequency (or mass deposited) were simultaneously monitored as a function of time for a series of pyrrole concentrations ranging over an order of magnitude from 0.01 to 0.10 mol dm^{-3} in 0.1 mol dm^{-3} TEATOS. From the

charge *vs.* time data the theoretical amount of material which should be deposited on the face of the mass sensing crystal can be calculated from a modified version of Faraday's law:

$$Q = nF\,\Delta m/M \qquad (3)$$

In this equation, n represents the number of moles of electrons required to deposit one mole of monomer units and thus can be viewed as an electropolymerization efficiency and M is the equivalent weight. Similarly, the frequency *vs.* time data yields the actual amount of material deposited at any time during electrolysis via the Sauerbrey equation. In order to relate frequency changes to changes in the number of moles of material deposited and thus determine the efficiency, two assumptions must be made. The first is the equivalent weight of the unit being deposited. The polymerization process is known to involve two electrons per molecule of pyrrole and since the polymer is produced in the charged or oxidized state, there will be another fraction of charge per pyrrole associated with the doping and incorporation of dopant counteranions. This fractional charge has been shown by many researchers to range from 0.2 to 0.5 [1, 30], or one counteranion for every 2 to 5 pyrroles depending on the anion and reaction conditions. This corresponds to an n-value of 2.2 to 2.5 electrons per pyrrole in the polymer chain. In this series of experiments, we have used a value of 0.39 tosylate anions per pyrrole, which was determined from elemental analysis on separate samples and is in good agreement with literature values [30]. Using the stoichiometric ratio shown in Structure 1, we can calculate an equivalent weight unit per pyrrole

Insert Structure 1

from the sum of the molecular weight of pyrrole, 65 g mol^{-1}, and the contribution from the tosylate counterion, 171 g mol^{-1} x 0.39, which yields a value of 132 g mol^{-1}. Any solvent incorporated along with the deposited species will result in an increase in the equivalent weight deposited and thus a decrease in the observed value for the number of electrons per pyrrole monomer unit.

The second assumption is that the rigid film approximation is valid which is necessary if the Sauerbrey equation is to be used to relate frequency to mass. One method of meeting the rigid film requirement is to limit the film thickness, ϵ, such that the relative mass loading, $\rho\epsilon/\rho_q l$, is less than 2%, where l = thickness of quartz [29]. When this condition is met the frequency change due to mass deposited will be negligible with respect to the resonant frequency of the unloaded quartz crystal and linear adherence to the Sauerbrey equation will be achieved. Using a typical frequency change of 40,000 Hz (corresponding to a 5 μm thick film) for poly(pyrrole tosylate), and deposition on a 5 MHz crystal, it can be seen that this lies well within the limits described by the rigid film approximation. These limits correspond roughly to a 10 μm thick film or a 80,000 Hz frequency change.

Experimental confirmation of our data can be seen by examining the typical plot of frequency and charge *vs.* time resulting from the potential step from 0.0 to 0.9 V applied to the electrode shown in Figure 3. It is seen that for the bulk of polymerization, both of these relationships are linear with time and not $t^{1/2}$ and thus the polymerization is not diffusion limited but is more likely controlled by the radical couplings of oxidized species. Current time plots do show an initial charging current, followed by a rising current which lasts on the order of 0.1 to 1.0 s due to nucleation. This time period is short in relation to the entire experiment and these phenomena are not observed in Figure 3. If we apply the modified Faraday's law, to the data in Figure 3, within the constraints of the equivalent weight per unit deposited described above (132 g mol^{-1}, Structure **1**), a plot of charge *vs.* moles of material deposited is obtained. The slope of this plot is proportional to n, the number of electrons per unit of pyrrole deposited. The plot shown in Figure 4 is taken from 1500 data points and has a slope proportional to 2.3 electrons/pyrrole with a value of 0.9998 for the square of the correlation coefficient (r^2). This is very strong additional evidence for adherence to the rigid film approximation for the polypyrrole system in solution.

To study the effects of pyrrole concentration on the polymerization efficiency, constant potential polymerizations were performed at 0.9 V in CH_3CN solutions containing 0.1 mol dm^{-3}

electrolyte and pyrrole concentrations ranging over an order of magnitude from 0.01 to 0.10 mol dm^{-3}. For each concentration of pyrrole, the effective n-value was determined at points during the polymerization where 50, 65, and 130 μg of poly(pyrrole tosylate) had been deposited in order to eliminate the possibility of effects that might occur from different film morphologies or density. The n-values were then plotted as a function of the pyrrole monomer concentration as shown in Figure 5. This plot indicates that low pyrrole monomer concentrations result in a decreased efficiency in the deposition process, independent of film thickness, as shown by a higher n-value. This will be discussed further.

Electrolyte Effects

A series of constant potential electrolyses were performed on solutions of acetonitrile (CH_3CN) and propylene carbonate (PC) containing 0.05 mol dm^{-3} pyrrole and 0.1 mol dm^{-3} TEATOS, $TBABF_4$ or $LiClO_4$ at potentials less than, equal to and greater than the oxidation potential, found for the pyrrole on the cyclic voltammogram of pyrrole monomer (Figure 2). To monitor deposition quantitatively, assumptions must again be made regarding the effective molecular weight of the species being deposited. From the literature values for dopant concentrations in bulk samples, we used a value of 87 g mol^{-1} when tetrafluoroborate (65 g mol^{-1} – 87 g mol^{-1} x 0.25) was the counteranion and 95 g mol^{-1} when perchlorate was used (65 g mol^{-1} + 99.5 g mol^{-1} x 0.30). Frequency, charge, and current *vs.* time plots, as described above, were obtained for each potential step experiment. Rising *i-t* relationships were observed which are similar to those discussed above and in References 3 to 7, however, the initial current spike corresponding to monolayer coverage was not seen in all cases which is probably due to a lack of sampling time resolution. The frequency and charge *vs.* time plots were again all linear for all polymerization conditions and the resulting charge *vs.* moles plots (for example, Figure 4, eqn. 3) yield a linear relationship with a correlation coefficient of greater than 0.99. The first derivative of this plot, dQ/dmol, is proportional to the n-value, or efficiency of polymerization, for any small increment of additional monomer added to the polymer film. The ability to measure n as

deposition proceeds allows us to monitor an effective efficiency of the polymerization/deposition as a function of polymer deposited. Typical plots for 0.05 mol dm^{-3} pyrrole in various solvent/electrolyte combinations are shown in Figures 6 and 7. These plots are not linear and indicate that there is a disproportionately high or low n-value (or polymerization efficiency) during the initial stages of polymerization followed by a rise or decay to a constant value. Also, some electrolyte/solvent combinations yielded overall n-values below the expected range of 2.2 to 2.5.

DISCUSSION

Effect of Pyrrole Concentration

The n-value vs. concentration data shown in Figure 5 has several important implications regarding both the nature of the polymerization process and the properties of the resulting films. The first is that, at a given potential, the efficiency of the polymerization process is dependent on the concentration of pyrrole in solution. This must be taken into account within the calculations used to determine film thicknesses by coulometric methods. This technique is often used in ionic diffusion and charge transport studies, as well as calculations routinely performed to determine dopant levels from the charge passed during a CV of the polymer film. A review of the literature shows values for charge passed to thickness ratios during film formation range from 0.38 to 400 mC μm^{-1} cm^{-2} [31]. This wide range of values indicates that only measuring the amount of charge passed to synthesize a given film is a poor way of estimating the amount and thickness of material actually deposited. In studies of charge transport, ion movement, and ion exchange in an electrochemically prepared film, ionic diffusion coefficients are often reported as a function of film thickness and, therefore, care must be taken when comparing these values between different polymer films formed under even slightly different polymerization conditions.

Using the mass change (determined from Sauerbrey's equation), the flotation density of poly(pyrrole tosylate), and the charge passed for a polymerization performed in highly efficient conditions (0.1 mol dm^{-3} TEATOS, 0.05 mol dm^{-3} pyrrole, CH_3CN, 0.9V), a minimal value of 233 mC cm^{-2} is appropriate to obtain a 1μm thick film. It should be noted that, at lower pyrrole

concentrations, a value of 700 mC cm^{-2} was obtained using the data for inefficient conditions (0.1 mol dm^{-3} TEATOS, 0.01 mol dm^{-3} pyrrole, CH_3CN, 0.9V).

Furthermore, a widely used method to calculate the dopant level in a given film is to compare the charge passed during polymerization to the charge necessary to fully oxidize a neutral film. This technique assumes each electron removed accounts for one doped site in the polymer and, thus, care must be taken because of the inefficiency of the electropolymerization and capacitive effects that occur during redox charging and discharging.

The dependence of the rate of polymerization on monomer concentration, or the order of reaction, can be studied from the slopes of the mass and charge *vs.* time plot during polymerization, Figure 3. These slopes will yield the rate of polymerization and deposition for any given concentration. The order of reaction has been studied by several researchers with somewhat conflicting results. A review of this literature yields values for the reaction order of 0 [32, 33], 1 [8, 13], and 1.5 [34] with respect to pyrrole concentration and a 0.5 pH order dependence in the case of polymerization on ITO glass. These values were obtained by examination of log i *vs.* log[pyrrole] plots as a function of potential during deposition. In all cases, the inefficiency due to loss of soluble oligomers to the bulk of solution and inability to separate the charge passed due to oxidative radical formation from that charge due to oxidation of the extended conjugation of the π backbone which results in the doped conducting material and capacitive charging is unaccounted for.

Using a microgravimetric technique avoids these ambiguities. Figure 8 shows a plot of the log of the deposition rate determined from mass-time slopes *vs.* log pyrrole concentration. A linear least squares fit of the data yields a slope of 2.04 . The electrochemically measured charge *vs.* time data can be handled in the same manner to yield a slope of 1.54, as shown in Figure 9. However, if the charge-time data is adjusted for the inefficiency at lower pyrrole concentrations using the data from Figure 6, the slope becomes equal to 1.94 . The rate dependence on the square of pyrrole concentration or a reaction order of two confirms, assuming only a small contribution from solvent

incorporation, that the rate limiting step during the bulk of polymerization is the coupling of the radical-cation species.

Electrolyte Effects

Figures 6 and 7 indicate that the efficiency of the electropolymerization process either increases or decreases relatively quickly to a stable value during film formation depending on the solvent used. Experiments like those shown were repeated several times at various potentials with highly reproducible results. Polymerizations in acetonitrile start out with a low efficiency and reach a stable value when approximately 1 μmol or about 1000 Å of polypyrrole have been deposited. Polymerizations in propylene carbonate start out with an excessively high efficiency that decreases quickly to a stable value when approximately 200 Å of polypyrrole has been deposited. The following facts emerge from this data. 1) The final and overall values of efficiency are electrolyte dependent, as illustrated in Table 1. 2) The leveling of the efficiency occurs well after polymer monolayer coverage but before the leveling of the current , i.e. during the nucleation and surface phase growth. 3) The increase or decrease to a constant value of efficiency is solvent dependent.

In addition, at potentials high enough for monomer oxidation to occur (starting at the foot of the cyclic voltammogram in Figure 2), the efficiency of the polymerization is independent of electrode potential.

The deviation of the ultimate value of n below a value of 2 for $TBABF_4$ in both CH_3CN and propylene carbonate and $LiClO_4$ in propylene carbonate may arise from incorporation of solvent into the polymer matrix. Table 1 lists the overall n-values determined from the slope of a linear squares fit of charge *vs.* moles of pyrrole deposited. The plots had excellent correlation coefficients and thus should reflect the overall state of the film. The n-values that are below the theoretical values suggest gross deviations in the film morphology and resulting incorporation of solvent into the polymer matrix. The dependence of the morphology and electroactive behavior on anion identity in polypyrrole films is well documented [35-40] with large aromatic dopant anions, such as tosylate, giving the best conductivities, stabilities, and mechanical properties, as well as the

most consistent morphologies. We have calculated the MW of the deposited unit from the MW of pyrrole and the MW and fraction of dopant anion found from bulk elemental analysis. In this manner additional solvent would lead to erroneously low values of n using the EQCM technique. One might argue that variations in solvent incorporation could lead to extreme variations in n-values seen in the initial phases of deposition in Figures 6 and 7. This possibility can be excluded because of opposite behavior exhibited by the two solvents studied.

We find that the rise or decay of n to a constant value is independent of the proposed monolayer coverage regimes measured electrochemically by Hillman [5] and Marcos [8] for polythiophene and polypyrrole respectively. Our experiment is not able to sample at short enough time scales to adequately measure the current spike that is characteristic of this step. Those results suggest that the competition between the formation of soluble oligomers and the nucleation process is the more important factor in the early period of film deposition. The solvent dependence of this phenomena also gives credence to the importance of oligomer solubility during the initial stages of film deposition. Thus, the following picture emerges for the initial stages of electropolymerization and deposition (see Scheme 2). The first step is the oxidation of the monomer to give a radical-cation which may couple with another radical cation to form a dimer species with a lower oxidation

Insert Scheme 2

potential than the monomer. The dimers formed in this step may undergo further oxidation and couple with other dimers or monomers which may remain soluble in the vicinity of electrode, diffuse away from the electrode, or participate in the formation of nucleation sites on the electrode surface. If the dimers/oligomers remain in the vicinity of the electrode they may be oxidized and continue to couple resulting in lower solubility and eventually precipitate as polymer. Diffusion away from the electrode results in coulombic inefficiency and a high n value. The differences seen by the two solvent systems probably stem from differences in the solubility of the dimer and oligomer species formed during the initial stages of electropolymerization. The PC system may be

allowing these initially formed oligomers to remain soluble, without diffusion into the bulk, until the point where they precipitate onto the electrode. This would yield the low n-value seen in the PC experiments for the time scale resolution available with EQCM system. This high efficiency is a result of sensing too large of a mass change from the QCM for the amount of charge passed. In our system, data is sampled every 200-250 msec; therefore, if we apply a potential step to the electrode, wait 250 msec, and then sample the frequency and current, it is possible to have failed to measure a significant amount of charge. However, the frequency change resulting from the oxidation and deposition of polypyrrole will be sensed. Once the electrode becomes covered by polymer film of sufficient thickness, the coulombic efficiency becomes stable. This suggests that once the electrode becomes highly nucleated and polymer growth is occurring in three dimensions. the primary radical coupling is between the radical cation monomer in solution and a radical polymer chain end within the polymer matrix.

CONCLUSIONS

Our conclusions from this EQCM study of the electropolymerization of pyrrole indicate that the polymerization efficiency during the film deposition is highly dependent on monomer concentration with low monomer concentrations yielding low efficiencies. There are also effects due to electrolyte and solvent although these are not as significant as monomer concentration. This inefficiency also indicates that measuring the charge passed to determine film thickness should be used with only a great deal of caution and should not be used when trying to compare films formed under different conditions. The rate of polymer deposition was found to be dependent on the square of the pyrrole monomer concentration and thus the electrochemical polymerization rate is limited by the radical coupling step.

We are in agreement with other authors with regard to the nucleation and phase growth mechanism in the early stages of polymerization. We offer additional insight into the role of oligomer formation, solubility, and deposition. Although our experimental setup is unable to elucidate the formation of initial monolayer of polymer ($t < 250$ ms), we feel that subsequent

deposition has a contribution from both electrode bound polymer coupling with soluble radical species and from the precipitation of low MW polymer chains which remain in solution until the point where their solubility decreases.

ACKNOWLEDGMENTS

This work was supported in part by grants from the Defense Advanced Research Projects Agency (monitored by the Office of Naval Research) and the Petroleum Research Fund (monitored by the American Chemical Society). The oscillator/potentiostat circuit for the microbalance was donated by IBM Research Division, San Jose, CA.

REFERENCES

1. (a) A. Diaz, Chemica Scripta, 17 (1981) 145; (b) R. J. Waltman, A. F. Diaz and J. Bargon, J. Electrochem. Soc., 132 (1985) 631; c) A. D. Jenkins and V. T. Stannett, Prog. Polym. Sci., 12 (1986) 179; d) J. R. Reynolds, J. Mol. Elec., 2 (1986) 1; e) T. Skothiem (Ed.), Handbook of Conducting Polymers, Vol. I and Vol. II, Marcel Dekker, New York, 1986.

2. (a) G. Nagasubramanian, S. Di Stefano and J. Moacanin, J. Phys. Chem., 90 (1986) 4447; (b) S. E. Lindsey and G. B. Street, Synth. Met., 10 (1984/85) 67; (c) O. Nina, M. Hikita and T. Tamamura, Appl. Phys. Lett., 46 (1985) 444; (d) M. DePaoli, R. J. Waltman, A. F. Diaz and J. Bargon, J. Chem. Soc., Chem. Commun., (1984) 1015; (e) O. Niwa and T. Tamamura, J. Chem. Soc., Chem. Commun., (1984) 817; (f) G. Ahlgren and B. Krische, J. Chem. Soc., Chem. Commun., (1984) 946; (g) T. T. Wang, S. Tasaka, R. S. Hutton and P. Y. Lu, J. Chem. Soc. Chem. Commun., (1985) 1343; (h) F. F. Fan and A. J. Bard, J. Electro. Chem. Soc., 133 (1986) 301; (i) L. L. Miller and Q. X. Zhou, Macromolecules, 20 (1987) 1594; (j) T. Shimidzu, A. Ohtani, T. Iyoda and K. Honda, J. Chem. Soc., Chem. Commun., (1986) 1415.

3. A. R. Hillman and E. F. Mallen, J. Electroanal. Chem., 220 (1987) 351.

4. A. J. Downard and D. Pletcher, J. Electroanal. Chem., 206 (1986) 139.

5. R. E. Noftle and D. Pletcher, J. Electroanal. Chem., 227 (1987) 229.

6. M. Sluyters-Rehbach, J. H. O. J. Wisenberg, E. Bosco and J. H. Sluyters, J. Electroanal. Chem., 235 (1987) 259.

7. H. L. Marcos, I. Rodriguez, and J. Gonzalez-Velasco, Electrochim. Acta, 32 (1987) 1453.

8. E. M. Genies, G. Bidan and A. F. Diaz, J. Electroanal. Chem., 149 (1983) 101.

9. S. Asavapiriyanont, G. K. Chandler, G. A. Gunawardena and D. Pletcher, J. Electroanal. Chem., 177 (1984) 229.

10. S. Asavapiriyanont, G. K. Chandler, G. A. Gunawardena and D. Pletcher J. Electroanal. Chem., 177 (1984) 245.

11. A. J. Downard and D. Pletcher, J. Electroanal. Chem., 206 (1986) 147.

12. C. K. Baker and J. R. Reynolds, Polym. Preprints, 28 (1987) 284.

13. G. Zotti, C. Cattarin and N. Comisso, J. Electroanal. Chem., 235 (1987) 259.

14. P. G. Pickup and R. A. Osteryoung, J. Am. Chem. Soc., 106 (1984) 2294.

15. P. A. Poropatic, R. Toyooka and J. R. Reynolds, unpublished results.

16. (a) A. F. Diaz, J. I. Crowley, J. Bargon, G. P. Gardini and J. B. Torrance, J. Electroanal. Chem., 121 (1981) 355; b) J. L. Bredas, R. Silbey, D.S. Boudreaux and R.R. Chance, J. Am. Chem. Soc., 130 (1983) 6555; (c) J. Heinze, J. Mortensen, J. K., Müllen and R. Schenk, J. Chem. Soc., Chem. Commun., (1987) 701.

17. J. H. Kaufman, K. K. Kanazawa and G. B. Street, Phys. Rev. Lett., 53 (1984) 2461.

18. K. H. Kaufman, Unpublished results.

19. W. D. Hinsberg, C. G. Willson and K. K. Kanazawa, J. Electrochem. Soc., 133 (1986) 1448.

20. P. T. Varineau and D. A. Buttry, J. Phys. Chem., 91 (1987) 1292.

21. D. Orata and D. A. Buttry, J. Am. Chem. Soc., 109 (1987) 3574.

22. S. Bruckenstein and S. Swathirajan, Electrochim. Acta, 30 (1985) 851; b) O. Melroy, K. Kanazawa, J. G. Gordon II and D. Buttry, Langmuir, 2 (1986) 697; c) M. Benje, M. Eiermann, U. Pittermann and K. G. Weil, Ber. Bunsenges. Phys. Chem., 90 (1986) 435; d) R. Schumacher, A. Müller and W. Stöckel, J. Electroanal. Chem., 219 (1987) 311; e) M. R. Deakin and O. Melroy, J. Electroanal. Chem., 239 (1988) 321.

23. S. Bruckenstein and M. Shay, J. Electroanal. Chem., 188 (1985) 131.

24. E. Grabbe, R. P. Buck and O. R. Melroy, J. Electroanal. Chem., 223 (1987) 67.

25. a) R. Schumacher, G. Borges and K. K. Kanazawa, Sur. Sci., 163 (1985) L621; b) R. Schumacher, J. G. Gordon and O. Melroy, J. Electroanal. Chem., 216 (1987) 127.

26. J. R. Reynolds, N. S. Sundaresan, M. P. Pomerantz, S. Basak and C. K. Baker, J. Electroanal. Chem., submitted.

27. G. Sauerbrey, Z. Fur Phys., 155 (1959) 206.

28. (a) K. K. Kanazawa and J. G. Gordon, Anal. Chem., 57 (1985) 1770; (b) K. K. Kanazawa and J. G. Gordon, Anal. Chim. Acta, 175 (1985) 99.

29. K. K. Kanazawa, Private Communication.

30. K. T. Wynne and G. B. Street, Macromolecules, 19 (1985) 2361.

31. (a) A. F. Diaz and J. I. Castillo, J. Chem. Soc., Chem. Commun., (1980) 397; (b) A. F. Diaz and J. M. Vasquez Vallejo, IBM J. Res. Dev., 25 (1981) 42; (c) A. F. Diaz, J. I. Castillo, J. A. Logan and W.-Y. Lee, J. Electroanal. Chem., 129 (1981) 115; (d) A. Watanabe, M. Tanaka and J. Tanaka, Bull. Chem. Soc. Jpn., 54 (1981) 2278; (e) M. Salmon, A. F. Diaz, A. J. Logan, M. Krounbi and J. Bargon, Mol. Cryst. Liq. Cryst., 83 (1982) 265; (f) R. A. Bull, F.-R. F. Fan and A. J. Bard, J. Electrochem. Soc., 129 (1982) 1009.

32. J. Prejza, I. Lundström and T. Skotheim, J. Electrochem. Soc., 129 (1982) 1685.

33. B. L. Funt and S. V. Lowen, Synth. Met., 11 (1985) 129.

34. I. Rodriquez, M. L. Marcos, J. Gonzalez-Velasco, Electrochim. Acta, 32 (1987) 1181.

35. A. F. Diaz, J. I. Castillo, J. A. Logan, and W. Y. Lee, J. Electroanal. Chem., 129 (1981) 115.

36. M. Salmon, A. F. Diaz, A. J. Logan, M. Krounbi and J. Bargon, Mol. Cryst. Liq. Cryst., 83 (1982) 265.

37. L. F. Warren and D. P. Anderson, J. Electrochem. Soc., 134 (1987) 101.

38. P. Marque, J. Roncali and F. Garnier, J. Electroanal. Chem., 218 (1987) 107.

39. T. Shimidzu, A. Ohtani, T. Iyoda and K. Honda, J. Electroanal. Chem., 224 (1987) 123.

40. L. J. Buckley, D. K. Roylance and G. E. Wnek, J. Polym. Sci. Poly. Phys. Ed., 25 (1987) 2179.

TABLE 1

n-values obtained from the slope of charge *vs.* moles of pyrrole deposited plots. [a,b]

Solvent	Electrolyte		
	TEATOS	$TBABF_4$	$LiClO_4$
Acetonitrile	2.36	1.77[c]	2.17
Propylene Carbonate	2.25	1.84[c]	1.70[c]

[a]Constant potential polymerizations were performed at 0.9 V *vs.* $Ag/AgNO_3$ in 0.05 mol dm^{-3} pyrrole and 0.1 mol dm^{-3} electrolyte

[b]All plots had r^2 values of better than 0.99

[c]These low values suggest incorporation of solvent into polymer matrix

FIGURE CAPTIONS

Figure 1 Schematic of the electrochemical quartz crystal-microbalance.

Figure 2 Cyclic voltammogram for pyrrole (0.05 mol dm^{-3}) at the gold electrode on a quartz crystal using the EQCM system. The CH_3CN + TEATOS (0.1 mol dm^{-3}). Potential scan rate 0.01 V sec^{-1}.

Figure 3 Frequency and charge *vs.* time response curve obtained during the electropolymerization of 0.05 mol dm^{-3} pyrrole in 0.1 mol dm^{-3} TEATOS/CH_3CN. Note that frequency can be used to calculate mass via Sauerbrey's Equation (1).

Figure 4 Charge *vs.* moles of pyrrole deposited as determined by mass. By Faraday's law, the slope is proportional to nF. r^2=0.9998

Figure 5 Electrons per pyrrole as a function of pyrrole concentration with 50 (o), 65 (Δ), and 130 (□) μg of poly(pyrrole tosylate) deposited films. The potential steps were from 0.0 to 0.9 V.

Figure 6 Number of electrons per pyrrole vs. moles of pyrrole deposited for 0.05 mol dm^{-3} pyrrole monomer in 0.1 mol dm^{-3} CH_3CN electrolyte for potential steps from 0.0 to 0.9 V. a) 0.1 mol dm^{-3} TEATOS, b) 0.1 mol dm^{-3} $LiClO_4$, c) 0.1 mol dm^{-3} $TBABF_4$.

Figure 7 Number of electrons per pyrrole vs. moles of pyrrole deposited for 0.05 mol dm^{-3} pyrrole monomer in 0.1 mol dm^{-3} propylene carbonate electrolyte for potential steps from 0.0 to 0.9 V. a) 0.1 mol dm^{-3} TEATOS, b) 0.1 mol dm^{-3} $LiClO_4$, c) 0.1 mol dm^{-3} $TBABF_4$.

Figure 8 Log-log plot for concentration dependence of polymerization rate obtained from dMass/dtime results.

Figure 9 Log-log plot for concentration dependence of polymerization rate obtained from dCharge/dtime results.

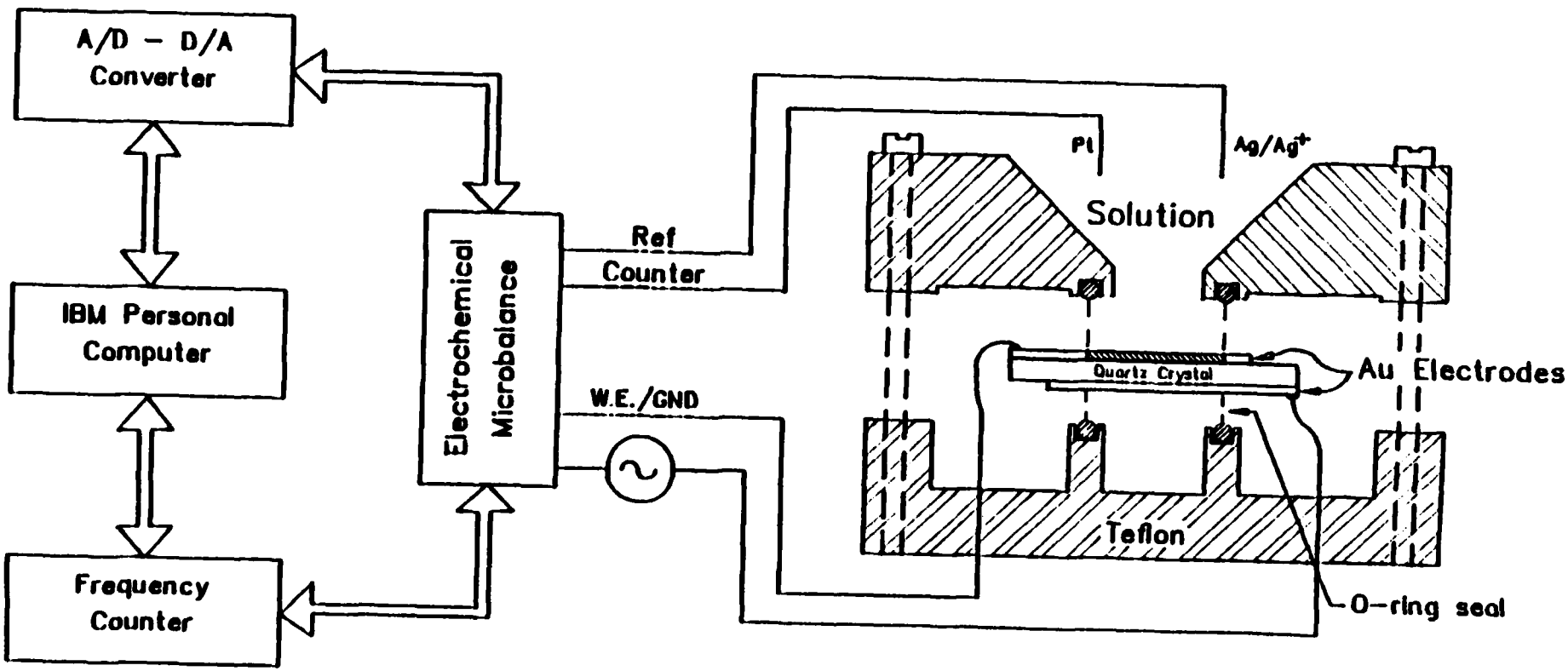
A/D – D/A
Converter
IBM Personal
Computer
Frequency
Counter
Electrochemical
Microbalance
Ref
Counter
W.E./GND
Pt
Ag/Ag+
Solution
Quartz Crystal
Au Electrodes
Teflon
O-ring seal

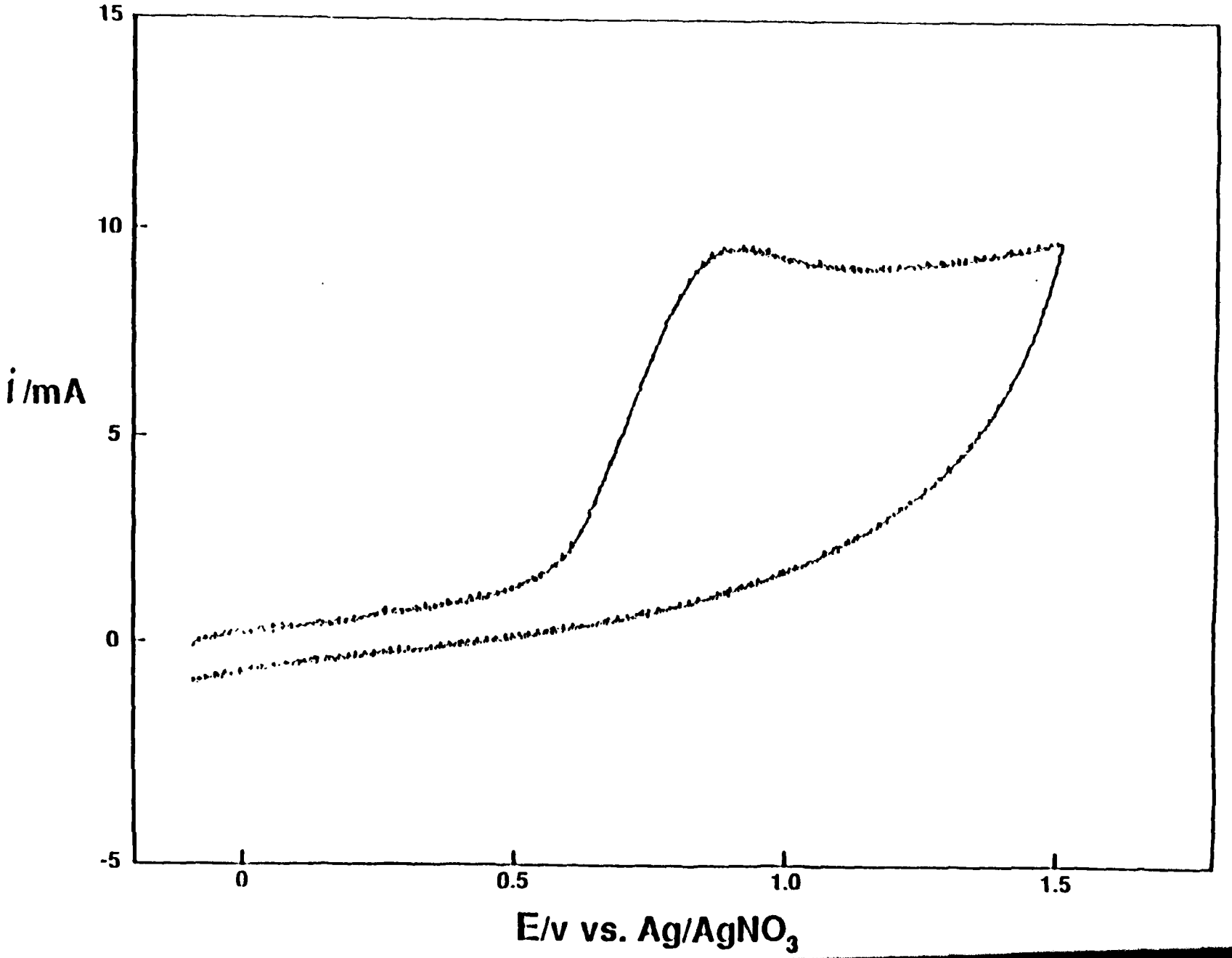
15
10
5
0
-5
i /mA
0
0.5
1.0
1.5
E/v vs. Ag/AgNO3

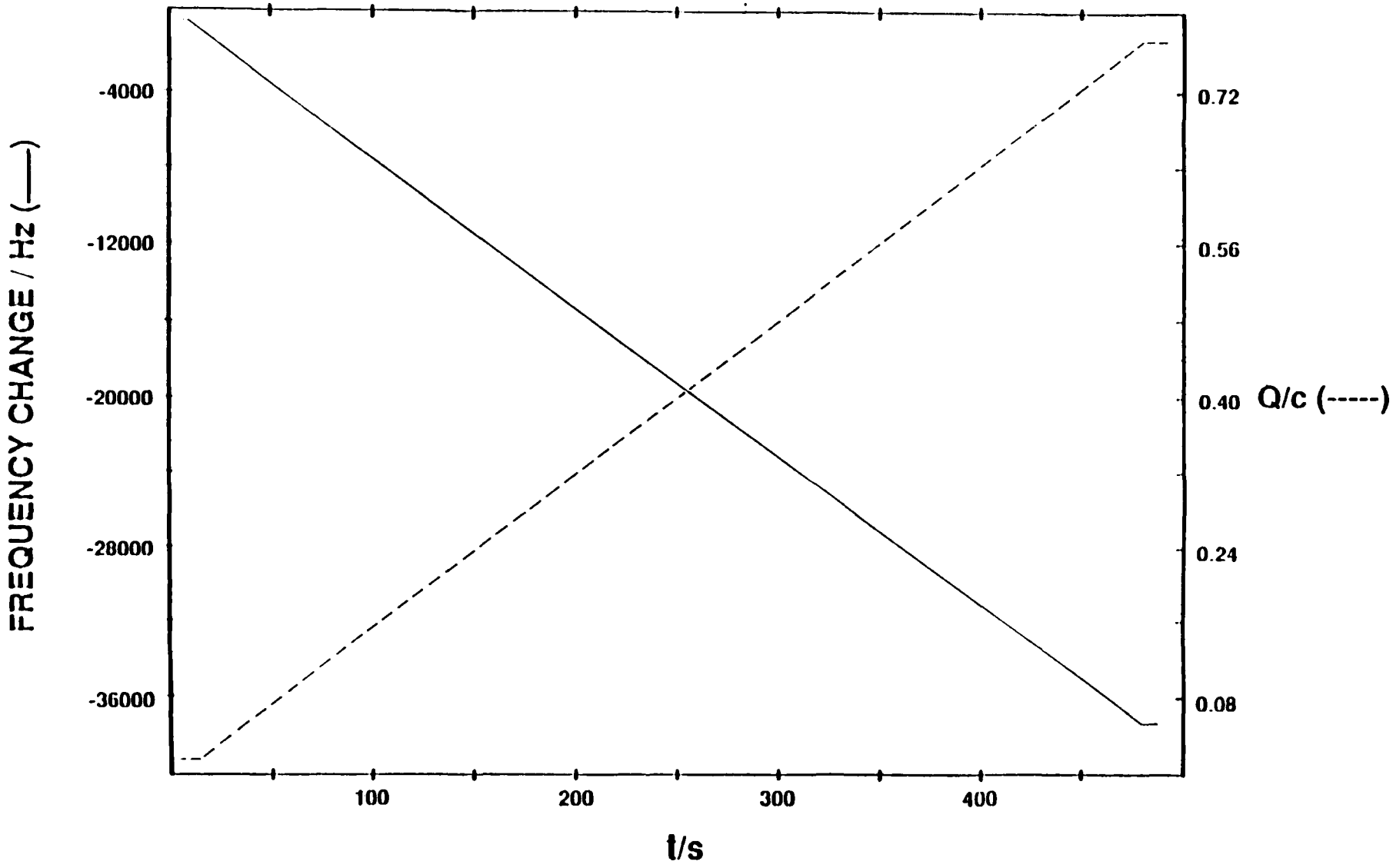
FREQUENCY CHANGE / Hz (——)
-4000
-12000
-20000
-28000
-36000
0.72
0.56
0.40
0.24
0.08
Q/c (-----)
100
200
300
400
t/s

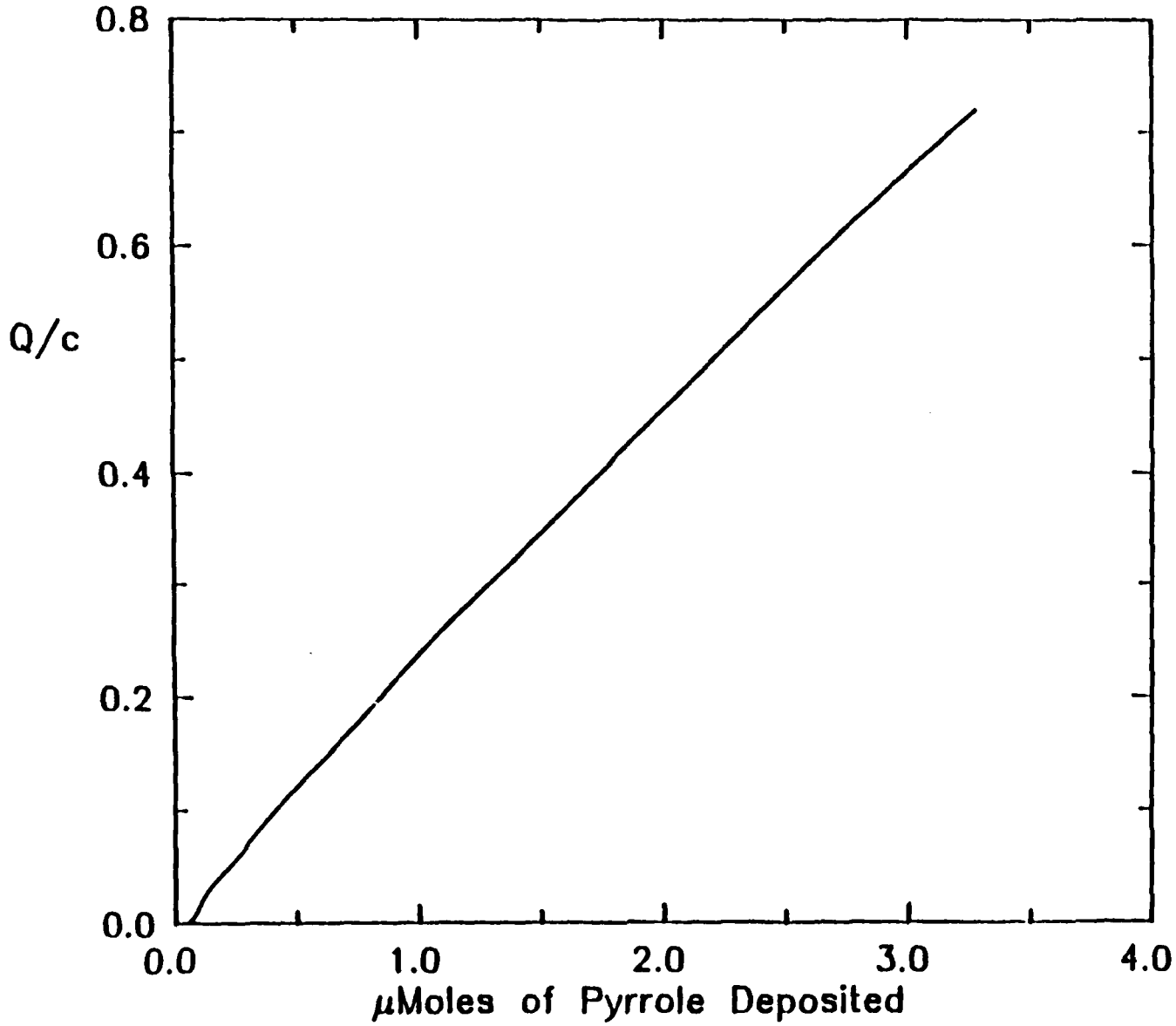
0.8
0.6
0.4
0.2
0.0
Q/c
0.0
1.0
2.0
3.0
4.0
μMoles of Pyrrole Deposited

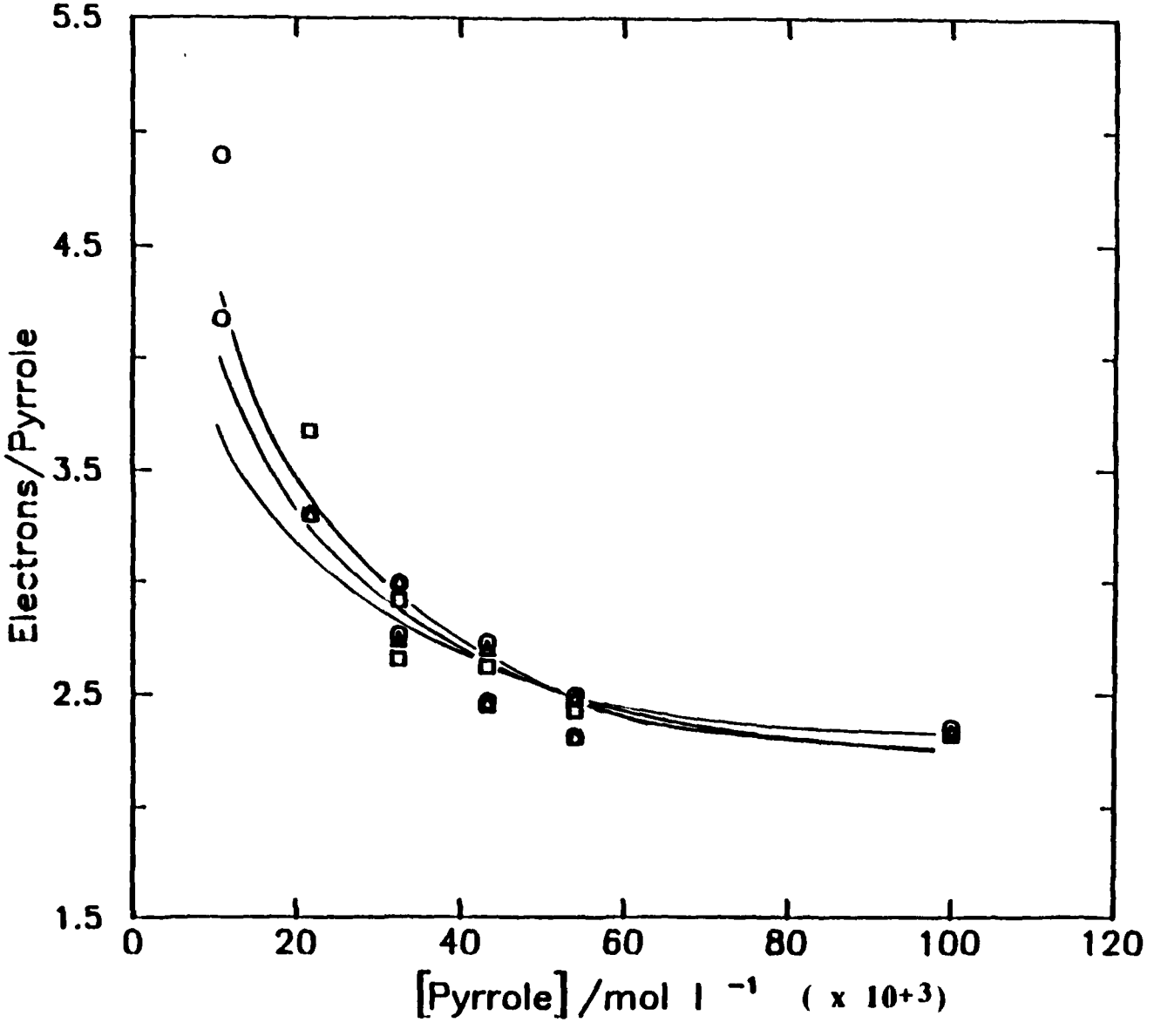
5.5
4.5
3.5
2.5
1.5
Electrons/Pyrrole
0
20
40
60
80
100
120
[Pyrrole] /mol l $^{-1}$ (x 10+3)

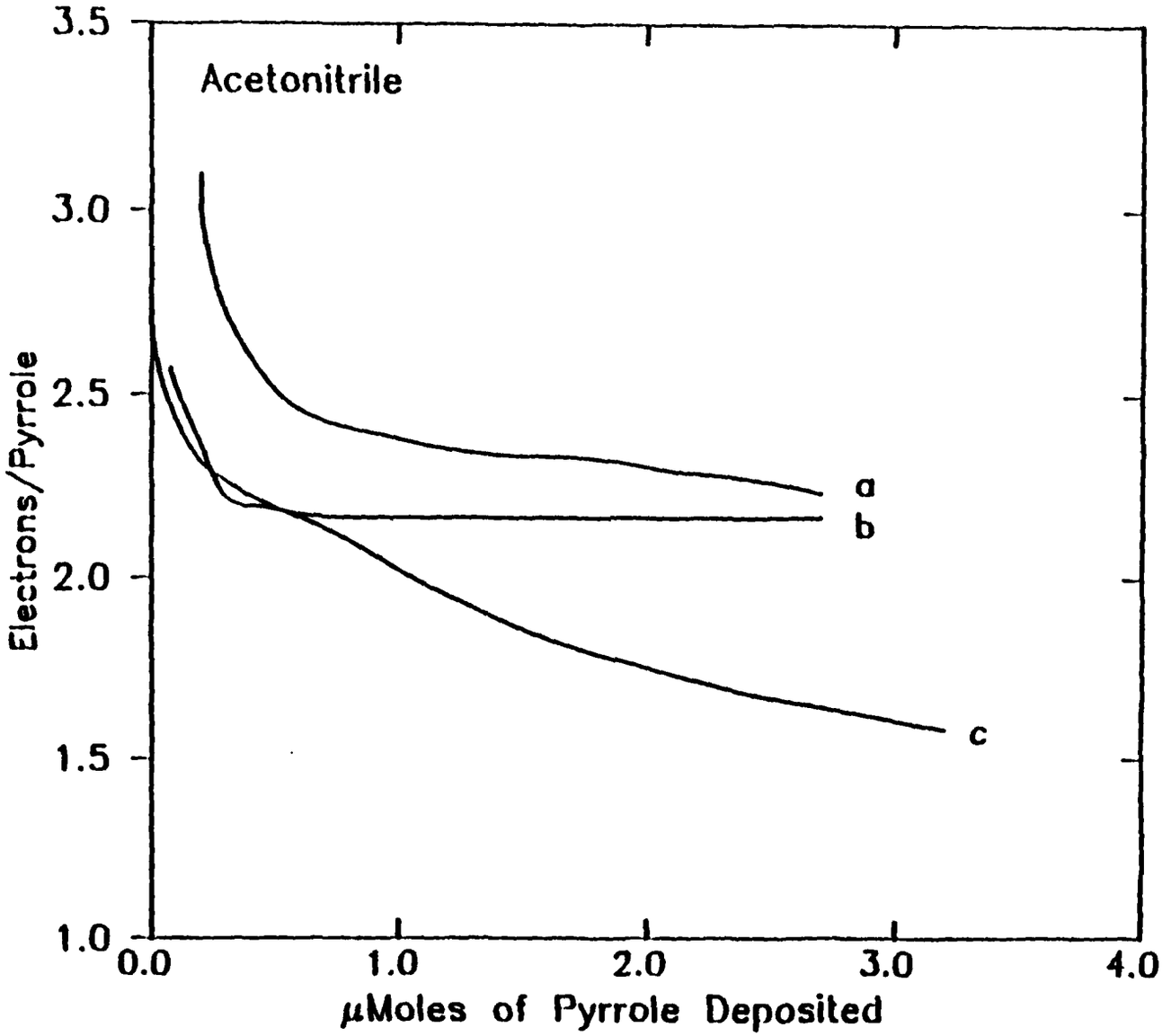
Acetonitrile
3.5
3.0
2.5
2.0
1.5
1.0
Electrons/Pyrrole
a
b
c
0.0
1.0
2.0
3.0
4.0
μMoles of Pyrrole Deposited

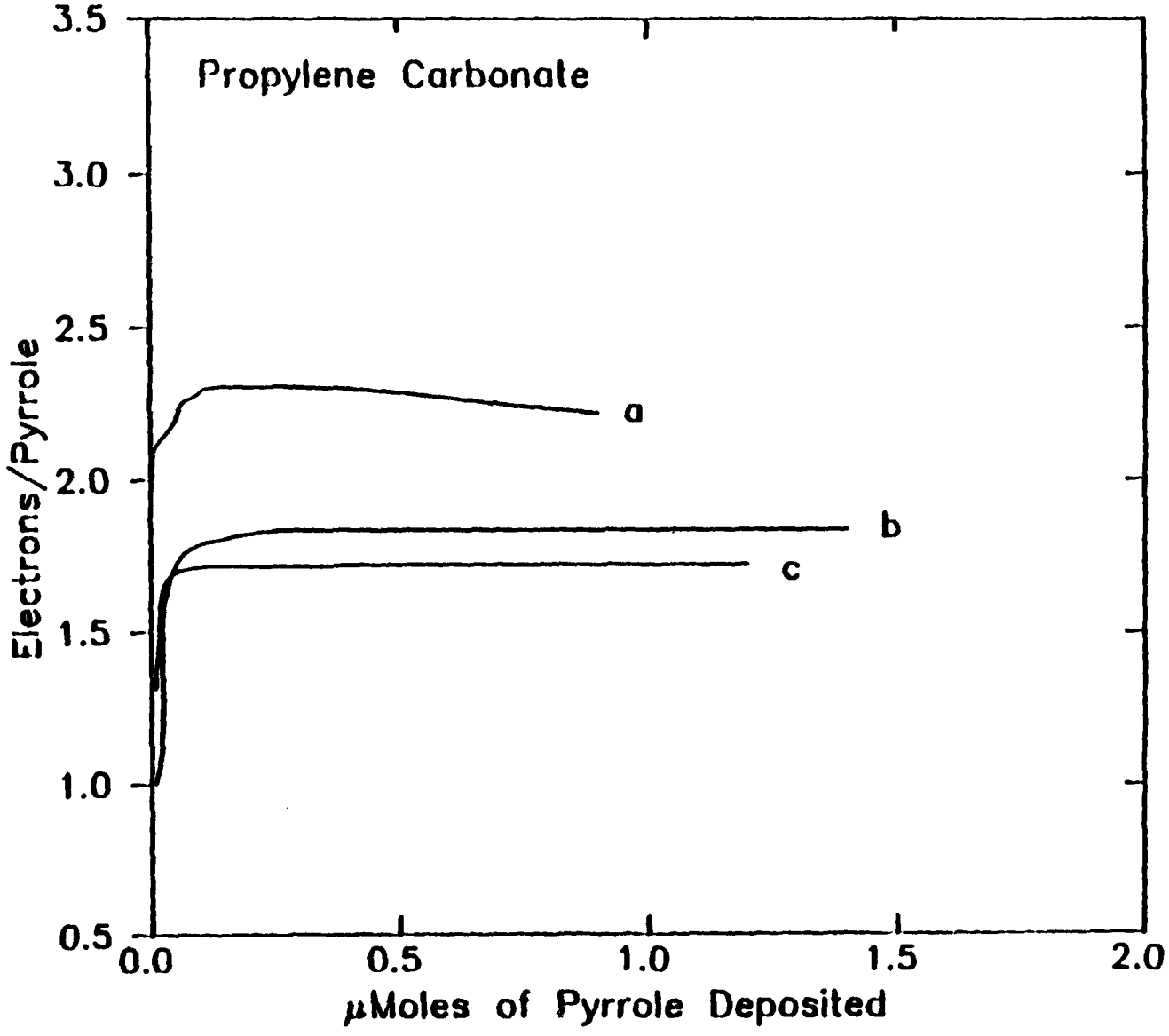
Propylene Carbonate
Electrons/Pyrrole
3.5
3.0
2.5
2.0
1.5
1.0
0.5
a
b
c
0.0
0.5
1.0
1.5
2.0
μMoles of Pyrrole Deposited

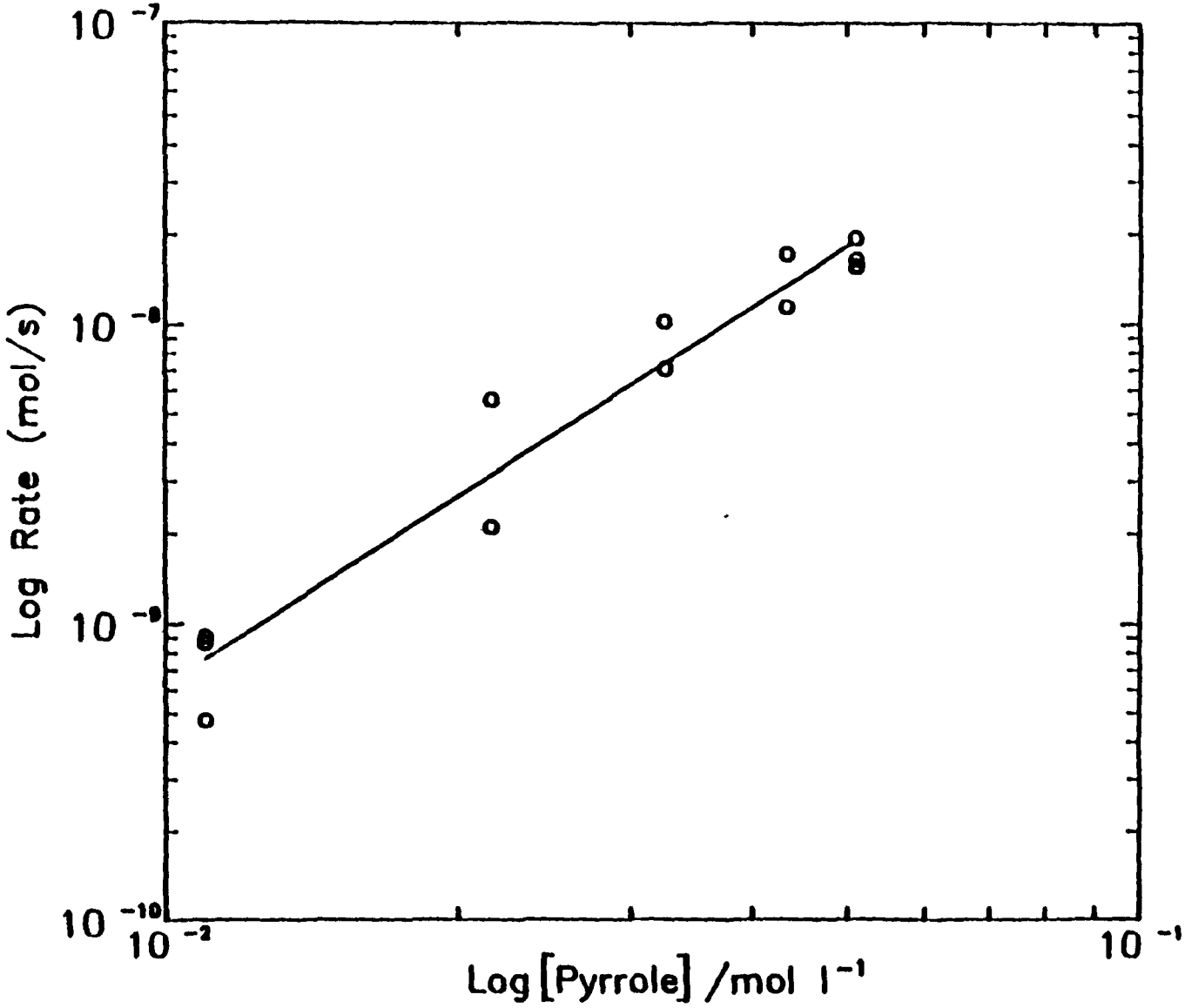
10 -7
10 -8
10 -9
10 -10
Log Rate (mol/s)
10 -2
10 -1
Log [Pyrrole] /mol l -1

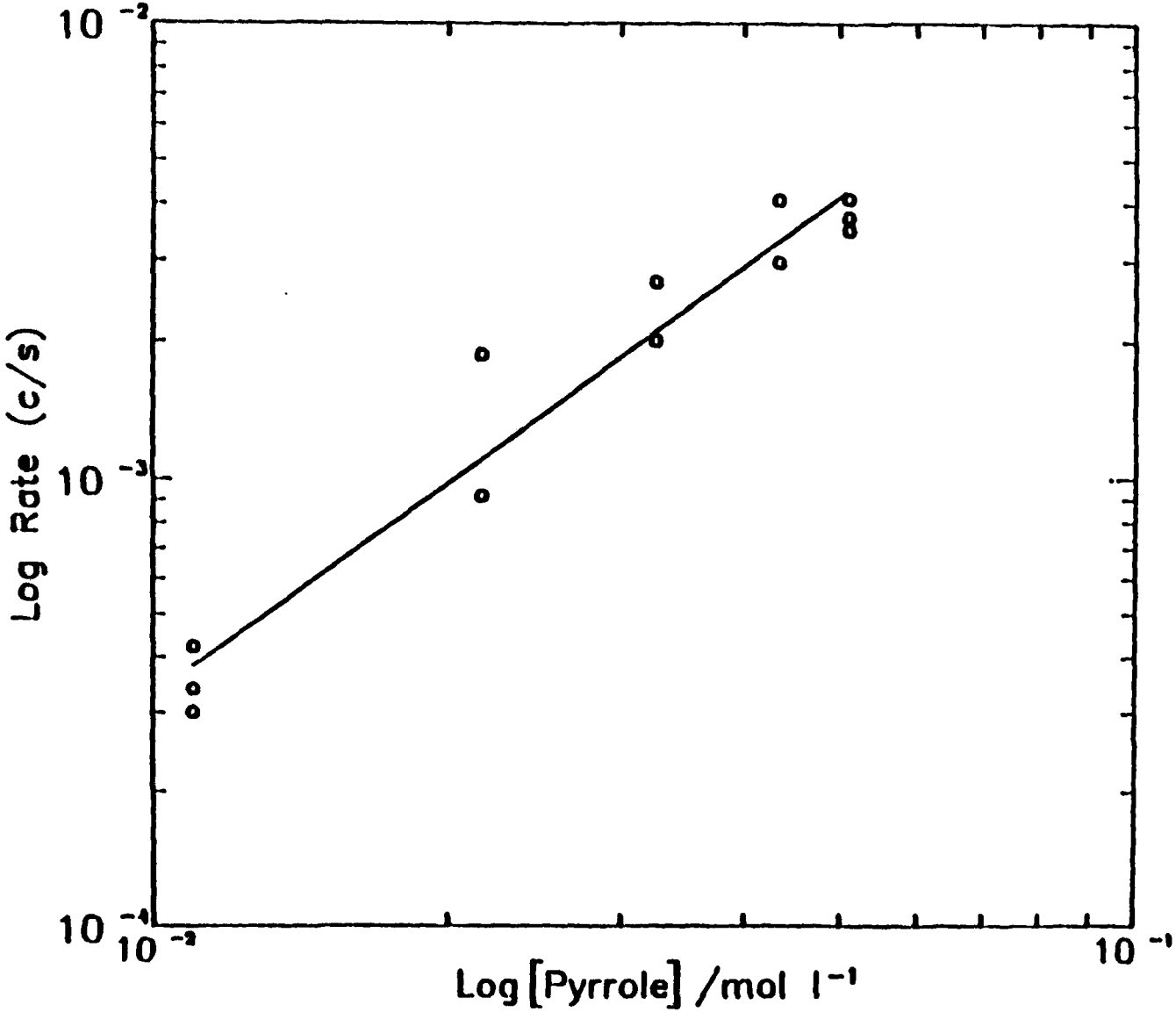
10 -2
10 -3
10 -4
Log Rate (c/s)
10 -2
10 -1
Log [Pyrrole] /mol l-1

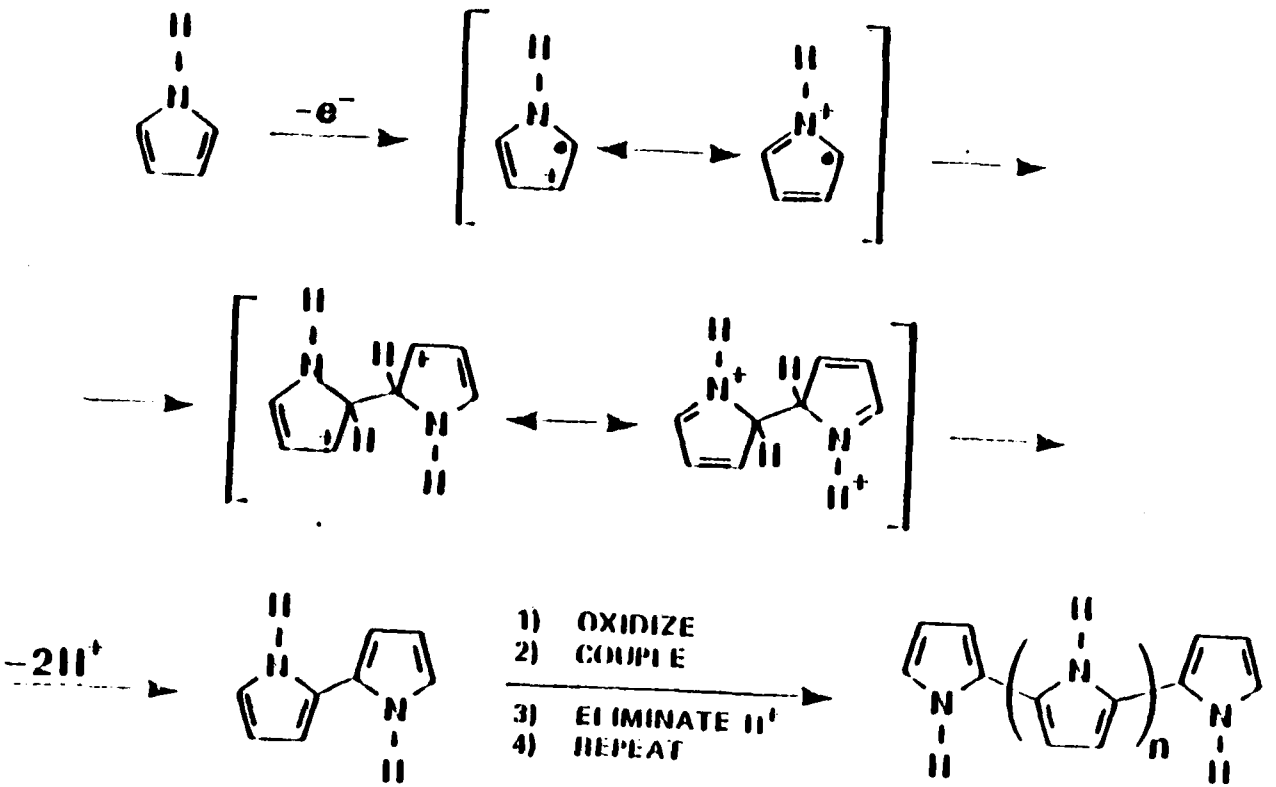

Scheme 1

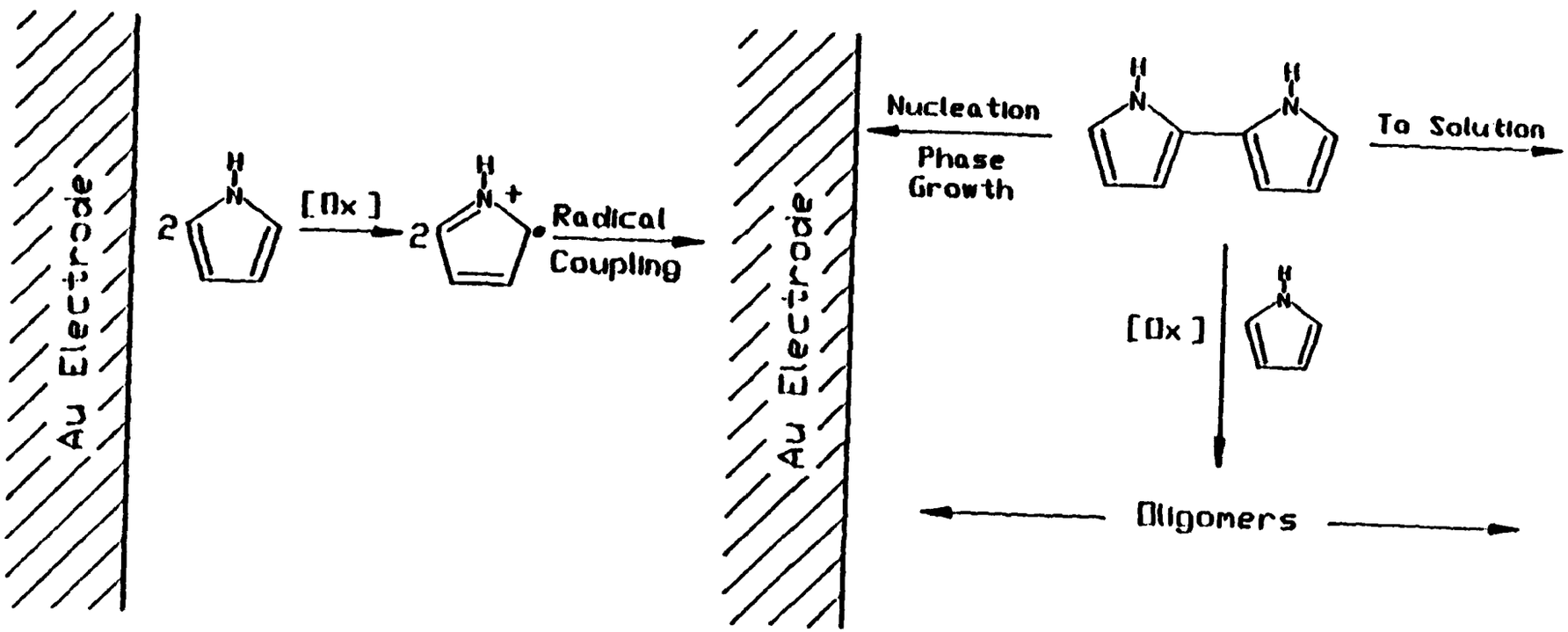
Au Electrode
2
[Ox]
2
Radical
Coupling
Au Electrode
Nucleation
Phase
Growth
To Solution
[Ox]
Oligomers

Scheme 2

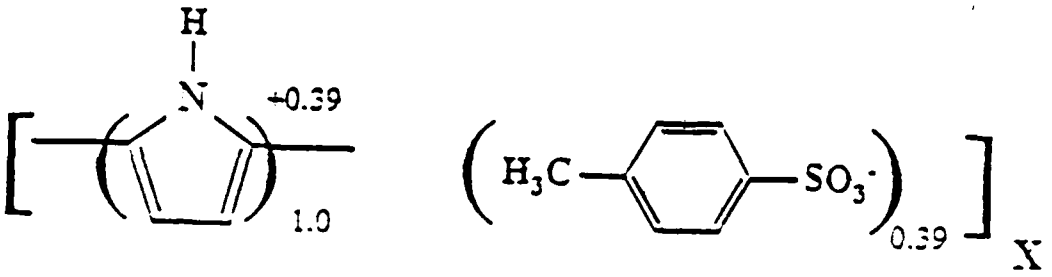

1